IOPscience iopscience.iop.org

Home Search Collections Journals About Contact us My IOPscience

Direct-write three-dimensional nanofabrication of nanopyramids and nanocones on Si by nanotumefaction using a helium ion microscope

This content has been downloaded from IOPscience. Please scroll down to see the full text.

2015 Nanotechnology 26 255303

(http://iopscience.iop.org/0957-4484/26/25/255303)

View the table of contents for this issue, or go to the journal homepage for more

Download details:

IP Address: 129.97.47.64
This content was downloaded on 04/06/2015 at 18:02

Please note that terms and conditions apply.

IOP Publishing Nanotechnology

Nanotechnology **26** (2015) 255303 (5pp) doi:10.1088/0957-4484/26/25/255303

Direct-write three-dimensional nanofabrication of nanopyramids and nanocones on Si by nanotumefaction using a helium ion microscope

L Zhang, N F Heinig, S Bazargan, M Abd-Ellah, N Moghimi and K T Leung

WATLab, and Department of Chemistry, University of Waterloo, Waterloo, Ontario N2L 3G1, Canada

E-mail: tong@uwaterloo.ca

Received 25 January 2015, revised 16 April 2015
Accepted for publication 24 April 2015
Published 4 June 2015

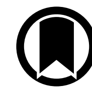

Abstract

The recently commercialized helium ion microscope (HIM) has already demonstrated its outstanding imaging capabilities in terms of resolution, surface sensitivity, depth of field and ease of charge compensation. Here, we show its exceptional patterning capabilities by fabricating dense lines and three-dimensional (3D) nanostructures on a Si substrate. Small focusing spot size and confined ion–Si interaction volume of a high-energy helium ion beam account for the high resolution in HIM patterning. We demonstrate that a set of resolvable parallel lines with a half pitch as small as 3.5 nm can be achieved. During helium ion bombardment of the Si surface, implantation outperforms milling due to the small mass of the helium ions, which produces tumefaction instead of depression in the Si surface. The Si surface tumefaction is the result of different kinetic processes including diffusion, coalescence and nanobubble formation of the implanted ions, and is found to be very stable structurally at room temperature. Under appropriate conditions, a linear dependence of the surface swollen height on the ion doses can be observed. This relation has enabled us to fabricate nanopyramids and nanocones, thus demonstrating that HIM patterning provides a new 'bottom-up' approach to fabricate 3D nanostructures. This surface tumefaction method is direct, both positioning and height accurate, and free of resist, etch, mode and precursor, and it promises new applications in nanoimprint mold fabrication and photomask clear defect reparation.

Keywords: direct-write nanofabrication, helium ion microscopy, nanocones and nanopyramids

(Some figures may appear in colour only in the online journal)

The advent of commercial helium ion microscope (HIM) in 2006 adds a new member to the microscope family for materials characterization and modification [1, 2]. HIM is very similar to a scanning electron microscope (SEM) except that it employs a helium ion beam as the illuminating particle source instead of an electron beam. The helium ions are produced by a gas field ion source, in which a high electric field exerted on the three topmost atoms (a trimer) of the tip causes field-ionization of approaching helium atoms. A trickle of helium ions, as born in a localized space of virtually atomic size, is placed in the center of the optical column as the particle source. The relatively massive helium ions have a much shorter de Broglie wavelength than electrons with the same energy, which reduces diffraction around the aperture and maintains a small focusing spot. The smaller energy and radial dispersions of helium ions alleviate chromatic and spherical aberrations, respectively, further improving the focusing spot. As a result, an ultimate focusing spot on the sample surface has been predicted to be as small as 0.25 nm [1], with a practical verifiable minimal focusing spot size of

 © 2015 IOP Publishing Ltd Printed in the UK

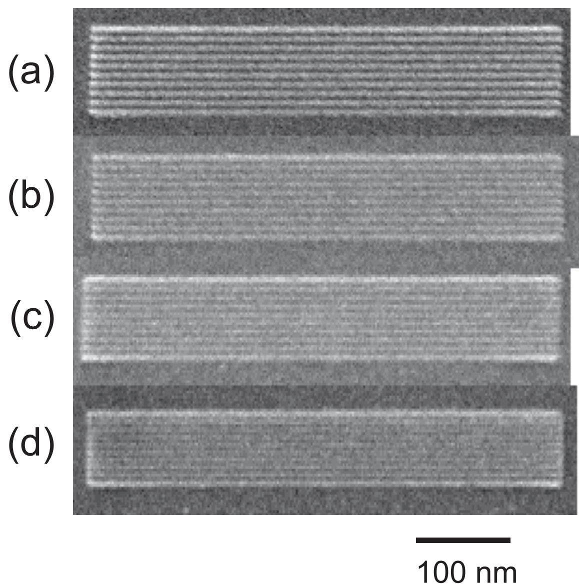

Figure 1. HIM images of sets of ten parallel lines (with a dose of 6×10^{10} ions cm^{-1} for each line) of 500 nm long with half pitch of (a) 5 nm, (b) 4 nm, (c) 3.5 nm and (d) 3 nm, all patterned with direct-write tumefaction technique in a HIM.

0.35 nm in a commercial instrument. In contrast, the resolution of a SEM is limited by a relatively large electron–substrate interaction volume than the focusing spot size. Comparing to electrons, the substrate interaction volume of helium ions is much smaller and more confined, especially closer to the surface where secondary electrons are generated and can be collected, because helium ions are less scattered near the surface inside the substrate. This has been shown in Monte Carlo simulations of electrons and helium ion interaction with Si [3, 4]. The smaller beam spots together with a smaller interaction volume have guaranteed important advantages in imaging by HIM over that by SEM: better resolution, higher surface sensitivity, and larger depth of field.

Like a gallium ion-based focus ion beam (FIB) microscope, HIM can also be used to directly modify a sample surface by sputtering (milling) and implantation, providing even smaller feature sizes than those achieved by FIB. Although helium ion bombardment has long been known to have a small sputter yield and cause metal surface blistering due to overdosed implantation, some recent publications show that HIM is capable of precision cutting (etching, milling) a variety of materials including graphene [5, 6], Au and Ni thin films [7, 8], SiN membranes [9], and ZnO nanotubes [10], with the attainable smallest milling feature size of 4 nm, which is significantly finer than a FIB-milled smallest feature size of typically 10 nm. The key to a successful cutting is that the sample must be thinner than the helium ion stopping range (~300 nm for 30 keV helium ions), which allows some of the incident helium ions to knock out substrate atoms (milling) or to undergo backscattering, with most of the ions passing through the film without accumulation. If the sample thickness is larger than the helium ion stopping range, the implanted helium ions will diffuse and coalesce to form clusters and bubbles, which induce swelling of the sample surface. Livengood *et al* studied subsurface damages of Si caused by helium ion bombardment as a function of dose and beam energy by cross-sectional transmission electron microscopy, and found that the accelerated helium ions lead to amorphous Si down to the ion stop depth, and nanobubbles occur above a dose threshold. These nanobubbles were found to be homogeneously distributed parallel to the Si surface and larger near the ion stop depth than near the surface, and they grew in size with increasing doses and caused the observed Si surface swelling [4]. It is believed that inside these nanobubbles are implanted He atoms. A similar study on neon ion-bombarded Si also revealed nanobubbles in cross-sectional TEM images, and an energy-dispersive x-ray analysis clearly indicated the presence of neon atoms inside the nanobubbles [11]. In spite of its high imaging resolution, the small sputter yields together with the implantation-induced swelling makes HIM unsuitable for circuit edit, because circuit edit involves milling from the backside of Si [12].

From our HIM patterning and imaging experiments on Si and subsequent height measurements of the HIM-patterned features by atomic force microscope (AFM), we observe that the swelling heights are proportional to the ion dose within an appropriate dose range, and the swollen surface appears smooth and stable. We can therefore take advantage of this linear height-dose relation to build three-dimensional (3D) nanostructures in a HIM. For example, by gradually increasing the dose when writing a square from the perimeter to the center, we can produce a nanopyramid of pre-defined dimensions. This new 3D nanofabrication technique (dubbed controlled tumefaction technique) is not only dry, but also precursor-, resist-, etch- and mold (stamp)-free, in marked contrast to other nanofabrication tools including nanoimprint lithography [13], nanotransfer printing [14], polyelectrolyte ink writing [15], and scanning probe lithography [16]. This technique promises applications for manufacturing 3D nanoobjects where the fine geometrical dimensions are of the most importance, such as a stamp used in nanoimprint lithography, which has been typically produced by repeated cycles of lithography and etching [13, 17].

By using an advanced nanopatterning tool incorporated into our HIM, we fabricate different nanostructures, including an array of closely placed parallel lines, nanopyramids and nanocones on Si surface using the aforementioned controlled tumefaction technique. We have further measured the heights of these 3D nanostructures by AFM to validate the technique.

An Orion plus HIM (Carl Zeiss SMT, Inc.) was used to perform the experiments. The microscope was operated with the extractor set at the so-called best imaging voltage typically near 35 kV, at which a source with the most brilliant trimer was obtained; a condenser lens spot control of 5; a beam-limiting aperture of 10 μm; a working distance of 5 mm; and a helium gas pressure of 2×10^{-6} mbar. At these settings, the beam current was about 1 pA. The beam spot is estimated to be 0.5 nm. An external Everhart–Thornley secondary electron detector was used for imaging. A pattern generator, Nanopatterning and Visualization Engine (NPVE) developed by Fibics Inc., was integrated into the Orion plus, which enabled

us to design the desired patterns and steer the helium beam to deliver the preset doses within the write field. Scanning of the helium beam was typically set to 0.25 nm per step, with a dwell time of 1.0 μs. Immediately after the pattern-writing process, images of the resulting pattern were collected with the HIM. The same sample was then measured with an AFM (Digital Instruments Dimension 3100 Nanoscope IV) in tapping mode. In order to facilitate positioning of the AFM tip to the patterned features, alignment markers (such as heavily dosed squares or letters) were made near the patterned features. These alignment markers could be easily located by using the CCD camera in the AFM. A p-type Si(100) chip ($2\times10\times0.5$ mm) with native oxide was used as the substrate, and it was cleaned with acetone and ethanol before introduction into the HIM.

Figure 1 shows HIM images of arrays of ten parallel lines of 500 nm long with pitch spacing of 10, 8, 7 and 6 nm, written by using NPVE with a dose of 6×10^{10} ions cm^{-1} for each line. All the lines with half-pitch spacing larger than 3.5 nm can clearly be resolved while those with a half-pitch of 3 nm are nearly resolved. These lines are found to be about 4 nm high by AFM. These tumefacted lines are the result of helium ion implantation into the Si substrates. The small size of helium atom facilitates its diffusion, coalescence and nanobubble formation. The smallest half pitch of HIM patterned lines reported to date is 4 nm on a 12 nm thick hydrogen silsesquioxane resist at a dose of 5.4×10^{8} ions cm^{-1} after development [17]. While the organic resist is apparently more sensitive than inorganic Si in terms of the doses needed for the HIM patterning, the required development process and secondary-electron-induced oversplash limit the smallest achievable features in a resist. In contrast, no other processes are needed on a bare Si substrate except for manipulating the dose, because secondary electrons have no influence on patterning. Although a swollen feature is generally expected to be less controllable than an indented one, we show here for the first time that the highest patterning resolution can still be achieved on Si, by taking advantage of the small helium beam spot, limited and confined helium ion scattering inside Si, and homogeneous distribution of helium nanobubbles parallel to the Si surface.

Figure 2(a) shows an image of a 5×5 μm square tumefacted slab, collected immediately after HIM-patterning with a 6×10^{16} ions cm^{-2} dose. The beam current for this patterning is 4.5 pA (written with HIM settings: 20 μm aperture, spot control 4, helium gas pressure 2×10^{-6} mbar). The beam spot is estimated to be a few nm and the patterning step size is 0.25 nm. The patterning process takes 9.5 min. Figure 2(b) displays an image of the same square slab taken 20 min later, during which period the helium ion beam was blanked so that no helium ions were exposed to the sample. Evidently, the darkened area inside the square slab immediately after patterning (figure 2(a)) becomes as bright as the unpatterned surface in 20 min (figure 2(b)), which suggests that a kinetic process has taken place during this time. No further change in the appearance and the overall cross-sectional shape of the square slab is observed with time, indicating that the material inside the square is in a stable or at least metastable state. The darkened area in figure 2(a) is caused by lower secondary electron yield related to structural/property changes of the material inside the square. This could be caused by sputtering (milling) of the Si surface by the helium ions. As shown by the AFM image in figure 2(c) and the corresponding height profile in figure 2(d), the square slab is a tumefacted object, with a height of 9.2 nm inside the square. The square surface is found to be generally smooth with a rms roughness of 0.9 nm, except at the taller perimeters (10.7 nm). The smooth swelling surface is due to homogeneously distributed helium nanobubbles parallel to the Si surface. Helium nanobubble formation and distribution can be seen in the cross-sectional TEM images of similar He ion implanted Si samples reported in [4]. Even considering the helium ion milling of the Si surface during the patterning process, the reduction in the vertical dimension has evidently been over-compensated by the tumefaction caused by the implanted helium atoms, which diffuse, coalesce and form nanobubbles at the stop depth within 20 min and lead to the homogeneous rise in the Si surface. The higher perimeter could be due to the redeposition of the sputtered Si atoms at the perimeters.

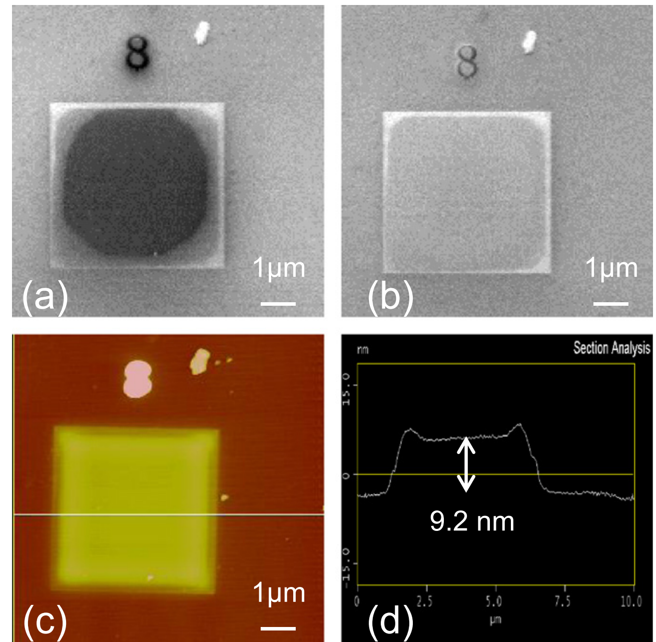

Figure 2. HIM images of HIM-patterned 5×5 μm square slab (with a dose of 6×10^{16} ions cm^{-2}) on a Si substrate collected (a) immediately and (b) 20 min after patterning with the helium ion beam blanked, and (c) the corresponding AFM topography image of (b), and (d) height profile of the square in (c).

We have further studied ion dose dependence of the tumefaction height of the square slab by patterning square slabs with different ion doses in HIM and measuring their heights with AFM. We find that above a threshold dose (1.2×10^{17} ions cm^{-2}), there exists a linear dependence of tumefaction height on the ion dose, with a slope of 31 nm rise per 1.0×10^{17} ions cm^{-2} dose increase (or 1920 nm rise per C cm^{-2} dose increase) for 1×1 μm square slabs (figure S1,

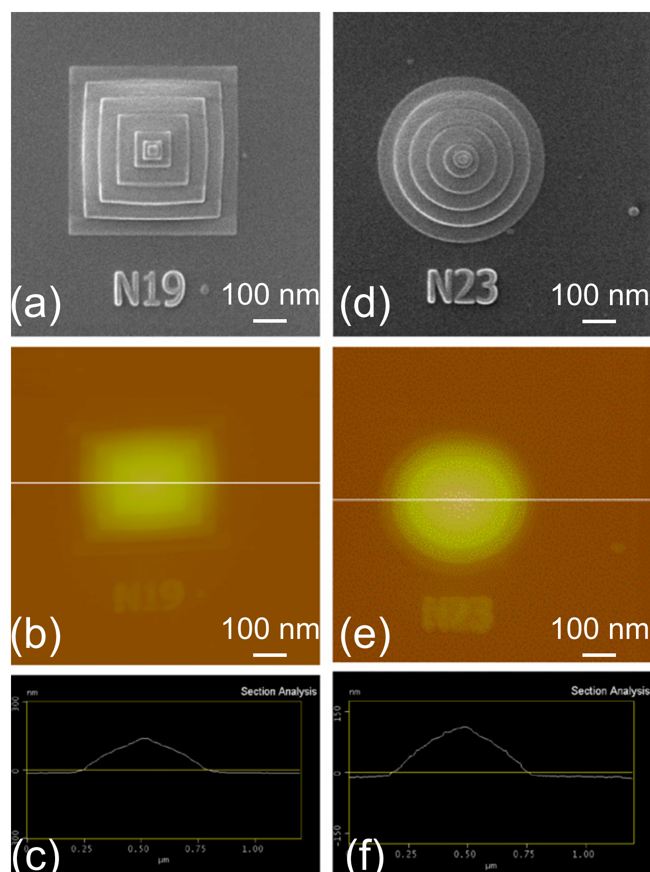

Figure 3. HIM images (top row), AFM images (middle row) and height profiles (bottom row) of (a)–(c) nanopyramid and (d)–(f) nanocone obtained by HIM-patterning with dose gradients.

supporting information)[1]. However, when the ion dose exceeds 1.2×10^{18} ions cm^{-2}, the perimeter of the square becomes distorted.

By taking advantage of the observed linear relation of tumefaction height versus ion dose, we proceed to fabricate nanopyramids and nanocones by gradually increasing the ion dose from the perimeter to the center of the square and circle, respectively. Figures 3(a) and (d) display HIM images of such patterned nanopyramid and nanocone, respectively. To obtain this nanopyramid, we first pattern a 500×500 nm square with a void (unexposed) concentric 400×400 nm square. The delivered dose is 1.8×10^{17} ions cm^{-2}, and the first step of the nanopyramid with 50 nm width is created. (Because no helium ions are delivered into this concentric 400×400 nm square, such a structure is technically called a void concentric square.) We then pattern a 400×400 nm square with a void concentric 300×300 nm square with a higher dose of 3.0×10^{17} ions cm^{-2}. This produces the second step of the nanopyramid with 50 nm width. We continue this process three more times, with 4.2×10^{17}, 5.4×10^{17}, and 6.6×10^{17} ions cm^{-2} doses for, respectively, the 300×300 nm, 200×200 nm, and 100×100 nm squares, each with a void concentric square of appropriate dimensions. Finally, we finish the nanopyramid by patterning a 50×50 nm solid square with a 7.8×10^{17} ions cm^{-2} dose at the center. Using a similar approach, we obtain nanocones by replacing the square base pattern with a circle base pattern. AFM measurements, shown in figures 3(b)–(f), confirm the formation of the nanopyramid and nanocone. The side planes of the nanopyramid and nanocone are relatively smooth. The heights of the nanopyramid and the nanocone are 151 nm (7.8×10^{17} ions cm^{-2} for the last solid square) and 120 nm (6.0×10^{17} ions cm^{-2} for the last solid circle), respectively. We have also employed another recipe to construct the nanopyramid, which is to pattern first a 500×500 nm solid square, then pattern concentrically a progressively smaller solid square (from 400×400 nm to 300×300 nm to 200×200 nm and to 100×100 nm) with the same or higher dose. This recipe is however less desirable because the resulting nanopyramid is found to have rough side planes, possibly due to a repetitive patterning at the same area.

In separation experiments, we also investigate the thermal stability of some tumefaction patterns ($10 \times 10\,\mu$m, $8 \times 8\,\mu$m, $5 \times 5\,\mu$m and $3 \times 3\,\mu$m square slabs) by either leaving them in air at room temperature for 45 days or annealing them after patterning at different temperatures for 10 min in flowing N_2. AFM measurements were performed to examine the height and shape changes of these tumefaction patterns. It is found that both the heights and height profiles of these square slabs exhibit no change after 45 days of storage in air at room temperature, indicating that these helium ion implanted structures are very stable at room temperature. On the other hand, heat treatment gives rise to significant changes to their shapes and heights. At 300 °C anneal, the heights of these square slabs rise by 10%, but their height profiles remain essentially unchanged, i.e. smooth centers with a higher perimeters. At 400 °C anneal, in addition to a further height increase, bubble formation is found in some square slabs, mostly at the center. At 500 °C anneal, those large tumefaction slabs ($10 \times 10\,\mu$m, $8 \times 8\,\mu$m) are all blown off, regardless of the exposure dose for these slabs before annealing. It is noteworthy that the explosion leaves behind a crater inside the square, the depth of which is ~350 nm and is dose-independent (figure S2, supporting information). This depth is in good agreement with the stop depth of the impinging helium ions with kinetic energy of 37 keV. This suggests that all the material inside the square above the stop depth has been removed together with the implanted He atoms. For the smaller tumefaction slabs ($5 \times 5\,\mu$m, $3 \times 3\,\mu$m), similar annealing treatment causes them to grow vertically into a dome in most cases (figure S3, supporting information), and sometimes they also break, leaving behind an irregularly shaped hole. The height of the dome increases with the annealing temperature, but the base of the dome does not exceed the size of its parent square slab. Since both the blown-off and the dome formation occur inside the original squares, the movement and impact of implanted He atoms during annealing proceed completely within the originally implanted volume.

In summary, we have demonstrated a new, simple 'bottom-up' approach of fabricating 3D nanostructures using a

[1] See supplementary material for details about dependence of tumefaction height on the ion dose and thermal stability of tumefaction patterns.

HIM. By combining an extremely small helium ion beam spot with a confined helium ion beam to the Si interaction volume, we show that it is feasible to pattern lines on Si with a half pitch as small as 3.5 nm for the first time. We observe a linear dependence of Si surface tumefaction height on the helium ion dose (in an appropriate range of ion dose). By taking advantage of this linear relation, we fabricate high-quality 3D nanopyramids and nanocones. The present method does not require any precursors, as needed in electron or ion beam induced deposition and micromachining, or molecules, as required in self-assembled nanostructures, or inks, as used in direct writing methods. 3D nanofabrication is essentially achieved by direct-write with a helium ion beam and by precision-control of their implantation. The many advantages of this method include: direct beam write, high-precision positioning and height control, and totally free from use of resist, etching, mold, stamp and precursors. Furthermore, the patterning results and the quality of the nanostructures so generated can be inspected *in situ* at high resolution immediately. This technique promises new applications in nanoimprint mold fabrication, photomask clear defect reparation, and 3D nanofabrication where height control on nanometer scale is essential.

Acknowledgments

This work was supported by the Natural Sciences and Engineering Research Council of Canada. The Orion plus helium ion microscope was purchased with the support of Canada Foundation for Innovation and the Ontario Research Fund. We are grateful to Fibics, Inc. for their kind assistance and advice on various nanopatterning topics.

References

[1] Ward B W, Notte J A and Economou N P 2006 *J. Vac. Sci. Technol.* B **24** 2871–4
[2] Economou N P, Notte J A and Thompson W B 2012 *Scanning* **34** 83–9
[3] Postek M T, Vladar A, Archie C and Ming B 2011 *Meas. Sci. Technol.* **22** 024004
[4] Livengood R, Tan S, Greenzweig Y, Notte J and McVey S 2009 *J. Vac. Sci. Technol.* B **27** 3244–9
[5] Bell D C, Lemme M C, Stern L A and Marcus C M 2009 *J. Vac. Sci. Technol.* B **27** 2755–8
[6] Archanjo B S, Fragneaud B, Cancado L G, Winston D, Miao F, Achete C A and Medeiros-Ribeiro G 2014 *Appl. Phys. Lett.* **104** 193114
[7] Melli M, Polyakov A, Gargas D, Huynh C, Scipioni L, Bao W, Ogletree D F, Schuck P J, Cabrini S and Weber-Bargioni A 2013 *Nano Lett.* **13** 2687–91
[8] Wang Y, Boden S A, Bagnall D M, Rutt H N and de Groot C H 2012 *Nanotechnology* **23** 395302
[9] Yang J, Ferranti D C, Stern L A, Sanford C A, Huang J, Ren Z, Qi L-C and Hall A R 2011 *Nanotechnology* **22** 285310
[10] Abd-Ellah M, Moghimi N, Zhang L, Heinig N F, Zhao L, Thomas J P and Leung K T 2013 *J. Phys. Chem.* C **117** 6794–9
[11] Tan S, Livengood R, Shima D, Notte J and McVey S 2010 *J. Vac. Sci. Technol.* B **28** C6F15–6F21
[12] Livengood R H, Winer P and Rao V R 1999 *J. Vac. Sci. Technol.* B **17** 40–3
[13] Li M, Chen L and Chou S Y 2001 *Appl. Phys. Lett.* **78** 3322–4
[14] Zaumseil J, Meitl M A, Hsu J W P, Acharya B R, Baldwin K W, Loo Y-L and Rogers J A 2003 *Nano Lett.* **3** 1223–7
[15] Gratson G M, Xu M and Lewis J A 2004 *Nature* **428** 386
[16] Pires D, Hedrick J L, De Silva A, Frommer J, Gotsmann B, Wolf H, Despont M, Duerig U and Knoll A W 2010 *Science* **328** 732–5
[17] Li W-D, Wu W and Williams R S 2012 *J. Vac. Sci. Technol.* B **30** 06F304